

# Quark-Hadron Phase Transitions in Young and Old Neutron Stars

A. Steiner, M. Prakash, and J.M. Lattimer

*Department of Physics & Astronomy, SUNY at Stony Brook, New York 11794-3800*

(February 9, 2020)

## Abstract

The mixed phase of quarks and hadrons which might exist in the dense matter encountered in the varying conditions of temperature and trapped neutrino fraction in proto-neutron stars is studied. The extent that the mixed phase depends upon the thermodynamical parameters as well as on the stiffness of matter in the hadronic and quark phases is discussed. We show that hadronic equations of state that maximize the quark content of matter at a given *density* generally minimize the extent of the mixed phase region in a neutron star of a given mass, and that only in extreme cases could a pure quark star result. For both the Nambu Jona-Lasinio and MIT bag quark models, neutrino trapping inhibits the appearance of a mixed phase which leads to possible proto-neutron star metastability. The main difference between the two quark models is the small abundance of strange quarks in the former. We also demonstrate that  $\partial T/\partial n < 0$  along adiabats in the quark-hadron mixed phase, opposite to what is found for the kaon condensates-hadron mixed phase. This could lead to core temperatures which are significantly lower in stars containing quarks than in those not containing quarks.

PACS: 97.60.Jd, 21.65.+f, 12.39.Fe, 26.60.+c

It has been proposed by several authors [1–3] that a mixed phase of hadrons and deconfined quarks might exist in the high density interior of neutron stars. The quark-hadron transition is being probed in relativistic heavy-ion collisions [4], but observations of neutron stars, in which matter is considerably less energetic, might also provide evidence of its existence. In this work, we analyze the structure of young and old neutron stars that contain quarks and indicate what effect quarks might make on observations, in particular, observations of neutrino emissions.

When a neutron star is born, the neutrinos produced by electron capture in the beta-equilibrated matter are prevented by their short mean free paths from leaving the star on dynamical timescales. The number of leptons per baryon that remain trapped is approximately 0.4, the precise value depending on the efficiency of electron capture reactions during the gravitational collapse of the progenitor star. On a timescale of 10–20 seconds, the neutrinos diffuse from the star, but leave behind much of their energy which causes significant heating of the ambient matter [5,6]. Entropies per baryon of about 2 (in units of the Boltzmann constant  $k_B$ ), and temperatures in the range 30–50 MeV, are generally achieved in the inner 50% of the star’s core at the peak of the heating. This is to be compared to entropies of approximately 1 which exist in the initial configuration. Following the heating, the star cools by radiating neutrino pairs of all flavors, and temperatures fall to below 1 MeV within minutes. Recent calculations [7,8] have verified this general scenario for a variety of equations of state (EOS) and assumptions about the composition of high-density matter.

Compared to cold neutron stars, the appearance of quarks is suppressed in a proto-neutron star (PNS) because of its high lepton number content. As the neutrinos leak out of a PNS, however, the central density of the star increases and the threshold density for the appearance of quarks decreases. Previous studies [3] have shown that the maximum mass supported by neutrino-rich matter is larger than that supported by neutrinoless matter if quarks appear. This gives rise to the possibility that some PNSs might become metastable [9–11], which would occur if the PNS mass lies within this range of maximum masses. When the maximum mass decreases below the PNS mass, after most of the neutrinos have diffused from the star, a collapse to a black hole ensues.

It is an open question whether or not the appearance of quarks could produce an observable effect in the light curves of the emitted neutrinos. To date, studies of quarks in PNS evolution have ignored

finite temperature, and have been limited mostly to the MIT bag model of quarks and restricted models of hadronic interactions. The new features of our study are to 1) include both the effects of trapped neutrinos and finite temperature, 2) examine the role of the quark model by employing both the traditional MIT bag model and the Nambu Jona-Lasinio (NJL) quark Lagrangian, 3) explore the effects of stiffness of the hadronic interactions on the quark-hadron transition, 4) study the effect of hyperons, and 5) delineate the phase diagram in the lepton number–baryon number density plane, appropriate for PNS studies.

To model the hadronic phase, we use a field-theoretical description, in which baryons interact via the exchange of  $\sigma$ -,  $\omega$ -, and  $\rho$ - mesons, extended to include hyperons. Specifically, we follow the approach of Müller and Serot [12] (hereafter MS). There is limited data which constrains the hadronic EOS at densities between nuclear matter equilibrium density and the density at which quarks become deconfined. Based on the considerations of “naturalness” in the context of an effective field theoretical approach, the Lagrangian gives a range of possible values for the couplings of higher order interactions between the vector mesons of the theory. We explore a range of these couplings in order to test the sensitivity of our results to variations in the stiffness of the hadronic supernuclear EOS. For densities lower than  $0.08 \text{ fm}^{-3}$ , we use the zero-temperature EOS of Negele and Vautherin [13], and for densities lower than  $0.001 \text{ fm}^{-3}$  we use the Baym-Pethick-Sutherland zero-temperature EOS [14]. Since the maximum mass and central densities of neutron stars depend only marginally on the low-density EOS, the assumption of zero-temperature for this low-density matter is satisfactory.

The MS Lagrangian is

$$\begin{aligned}
\mathcal{L} = & \sum_B \bar{B} (i\gamma^\mu \partial_\mu - g_{\omega B} \gamma^\mu \omega_\mu - g_{\rho B} \gamma^\mu \mathbf{b}_\mu \cdot \mathbf{t} - M_B + g_{\sigma B} \sigma) B \\
& - \frac{1}{2} m_\sigma^2 \sigma^2 + \frac{1}{2} \partial_\mu \sigma \partial^\mu \sigma - \frac{\kappa}{3!} \sigma^3 - \frac{\lambda}{4} \sigma^4 \\
& + \frac{1}{2} m_\omega^2 \omega^\mu \omega_\mu - \frac{1}{4} F_{\mu\nu} F^{\mu\nu} + \frac{\zeta}{4!} g_\omega^4 (\omega^\mu \omega_\mu)^2 \\
& + \frac{1}{2} m_\rho^2 \mathbf{b}^\mu \mathbf{b}_\mu - \frac{1}{4} \mathbf{B}_{\mu\nu} \mathbf{B}^{\mu\nu} + \frac{\xi}{4!} g_\rho^4 (\mathbf{b}^\mu \mathbf{b}_\mu)^2 + \mathcal{L}_\ell
\end{aligned} \tag{1}$$

where the sum over  $B$  is a sum over all nucleons and hyperons, and  $\mathcal{L}_\ell$  represents the sum of the Dirac Lagrangians for all of the leptons (electrons, muons and neutrinos). The values of  $\kappa$ ,  $\lambda$ ,  $g_{\rho N}$ ,  $g_{\sigma N}$ , and

$g_{\omega N}$  are set by matching the equilibrium nuclear density ( $n_0 = 0.16 \text{ fm}^{-3}$ ), binding energy ( $E_b = -16 \text{ MeV}$ ), compressibility ( $K_0 = 250 \text{ MeV}$ ), nucleon effective mass ( $M_0^* = 0.6M$ ), and symmetry energy ( $e_{sym} = 35 \text{ MeV}$ ) at  $n_0$ . The remaining two parameters,  $\xi$  and  $\zeta$ , associated with non-linear vector and isovector interactions, control the stiffness of the hadronic EOS at supernuclear densities. Larger values of either parameter tend to soften the EOS. The acceptable ranges for  $\zeta$  and  $\xi$ , based on considerations of naturalness, are  $0 \leq \xi \leq 1.5$  and  $0 \leq \zeta \leq 0.06$  [12].

We include the  $\Lambda$ ,  $\Sigma^+$ ,  $\Sigma^0$ ,  $\Sigma^-$ ,  $\Xi^0$ , and  $\Xi^-$  hyperons and ignore the heavier  $\Delta$  baryon which is too massive to affect our results. We assume that all six hyperon coupling constants with a particular vector meson are equal. Furthermore, the hyperon coupling constants are related to the nucleon–vector meson coupling constants by

$$g_{\sigma H} = x_\sigma g_{\sigma N}, \quad g_{\rho H} = x_\rho g_{\rho N}, \quad g_{\omega H} = x_\omega g_{\omega N}. \quad (2)$$

Following Glendenning and Moszkowski [15] we assume  $x_\rho = x_\sigma = 0.8$ . We also take  $x_\omega = 0.895$ , which follows from the binding energy,  $-28 \text{ MeV}$ , of the  $\Lambda$  hyperon in nuclei [16].

In the mean field approximation, the thermodynamic potential  $\Omega$  is given by (*cf.* [17])

$$\begin{aligned} \frac{\Omega}{V} = & \frac{1}{2}m_\sigma^2\sigma^2 + \frac{\kappa}{3!}\sigma^3 + \frac{\lambda}{4!}\sigma^4 - \frac{1}{2}m_\omega^2\omega_0^2 - \frac{1}{2}m_\rho^2b_0^2 - \frac{\zeta}{4!}g_\omega^4\omega_0^4 \\ & - \frac{\xi}{4!}g_\rho^4b_0^4 - \sum_B 2T \int \frac{d^3p}{(2\pi)^3} \ln(1 - f_B) + \Omega_\ell \end{aligned} \quad (3)$$

where the distribution function is  $f_B = [1 + \exp(\beta(E_B^* - \nu_B))]^{-1}$ . Here,  $\beta = 1/T$ , the effective chemical potential is  $\nu_B = \mu_B - g_{\omega B}\omega_0 - g_{\rho B}t_3b_0$ , the effective mass is  $M_B^* = M_B - g_{\sigma B}\sigma$ , and  $E_B^* = \sqrt{p^2 + M_B^{*2}}$ . The contribution of antibaryons is not significant for the thermodynamics of interest for a PNS and have been ignored. The contribution from the leptons,  $\Omega_\ell$ , is given adequately by its non-interacting form [18].

The thermodynamic potential of the quark phase is  $\Omega = \Omega_{\text{FG}} + \Omega_{\text{Int}}$ , where

$$\frac{\Omega_{\text{FG}}}{V} = -2N_c T \sum_{i=u,d,s} \int \frac{d^3p}{(2\pi)^3} [\ln(1 - f_i) + \ln(1 - \bar{f}_i)] \quad (4)$$

denotes the Fermi gas contribution arising from quarks. We consider three flavors,  $i = u, d, s$  and three colors,  $N_c = 3$  of quarks. The distribution functions of fermions and anti-fermions are  $f_i =$

$[1 + \exp(\beta(E_i - \mu_i))]^{-1}$  and  $\bar{f}_i = [1 + \exp(\beta(E_i + \mu_i))]^{-1}$ , where  $E_i$  and  $\mu_i$  are the single particle energy and chemical potential, respectively, of quark species  $i$ . To explore the sensitivity of the quark model, we contrast the results of the MIT bag and the Nambu Jona-Lasinio (henceforth NJL) models for  $\Omega_{\text{Int}}$ .

In the MIT bag model, the Fermi gas contribution is calculated using current, as opposed to dynamical, quark masses. The interactions between quarks inside the confining cavity (the bag) are taken to be perturbative. Thus,  $\Omega_{\text{Int}} = BV + \Omega_{ex} + \Omega_{corr} + \dots$ , where the constant  $B$  has the simple interpretation as the pressure of the vacuum (the so-called bag constant or bag pressure),  $\Omega_{ex}$  denotes the two-loop or one-gluon exchange contribution, and  $\Omega_{corr}$  represents higher order correlation contributions from ring diagrams, etc. [18] In this work, we will restrict ourselves to the simplest bag model and keep only the constant cavity pressure term. The results are qualitatively similar to what is obtained by including the higher order terms, if the bag constant  $B$  is slightly altered [19].

Several features of the Lagrangian of Quantum Chromo-Dynamics (QCD), including the spontaneous breakdown of chiral symmetry, are exhibited by the Nambu Jona-Lasinio (NJL) model, which shares many symmetries with QCD. In its commonly used form, the NJL Lagrangian reads

$$\begin{aligned} \mathcal{L} = & \bar{q}(i\not{\partial} - \hat{m}_0)q + G \sum_{k=0}^8 [(\bar{q}\lambda_k q)^2 + (\bar{q}i\gamma_5\lambda_k q)^2] \\ & - K [\det_f(\bar{q}(1 + \gamma_5)q) + \det_f(\bar{q}(1 - \gamma_5)q)] . \end{aligned} \quad (5)$$

The determinant operates over flavor space,  $\hat{m}_0$  is the  $3 \times 3$  diagonal current quark mass matrix,  $\lambda_k$  represents the 8 generators of SU(3), and  $\lambda_0$  is proportional to the identity matrix. The four-fermion interactions stem from the original formulation of this model [20], while the flavor mixing, determinantal interaction is added to break  $U_A(1)$  symmetry [21]. Since the coupling constants  $G$  and  $K$  are dimensionful, the quantum theory is non-renormalizable. Therefore, an ultraviolet cutoff  $\Lambda$  is imposed, and results are considered meaningful only if the quark Fermi momenta are well below this cutoff.

The coupling constants  $G$  and  $K$ , the strange quark mass  $m_{s,0}$ , and the three-momentum ultraviolet cutoff parameter  $\Lambda$ , are fixed by fitting the experimental values of  $f_\pi$ ,  $m_\pi$ ,  $m_K$  and  $m_{\eta'}$ . We use the values of Ref. [22], namely  $\Lambda = 602.3$  MeV,  $G\Lambda^2 = 1.835$ ,  $K\Lambda^5 = 12.36$ , and  $m_{0,s} = 140.7$  MeV, obtained using  $m_{0,u} = m_{0,d} = 5.5$  MeV. The subscript “0” denotes current quark masses. Results of

the gross properties of PNSs obtained by the alternative fits of Refs. [23] and [24] are similar to the results quoted below.

In the mean field approximation at finite temperature and at finite baryon density, the thermodynamic potential due to interactions is given by [24]:

$$\begin{aligned} \frac{\Omega_{\text{Int}}}{V} = & 2N_c \sum_{i=u,d,s} \int \frac{d^3p}{(2\pi)^3} \left( \sqrt{m_i^2 + p^2} - \sqrt{m_{0,i}^2 + p^2} \right) \\ & + 2G \langle \bar{q}_i q_i \rangle^2 - 4K \langle \bar{q}_u q_u \rangle \langle \bar{q}_d q_d \rangle \langle \bar{q}_s q_s \rangle . \end{aligned} \quad (6)$$

In both Eqs. (4) and (6) for the NJL model, the quark masses are dynamically generated as solutions of the gap equation obtained by requiring that the potential be stationary with respect to variations in the quark condensate  $\langle \bar{q}_i q_i \rangle$ :

$$m_i = m_{0,i} - 4G \langle \bar{q}_i q_i \rangle + 2K \langle \bar{q}_j q_j \rangle \langle \bar{q}_k q_k \rangle , \quad (7)$$

$(q_i, q_j, q_k)$  representing any permutation of  $(u, d, s)$ . The quark condensate  $\langle \bar{q}_i q_i \rangle$  and the quark number density  $n_i = \langle q_i^\dagger q_i \rangle$  are given by:

$$\begin{aligned} \langle \bar{q}_i q_i \rangle &= -2N_c \int \frac{d^3p}{(2\pi)^3} \frac{m_i}{E_i} [1 - f_i - \bar{f}_i] \\ n_i = \langle q_i^\dagger q_i \rangle &= 2N_c \int \frac{d^3p}{(2\pi)^3} [f_i - \bar{f}_i] . \end{aligned} \quad (8)$$

A comparison between the MIT bag and NJL models is facilitated by defining an effective bag pressure in the NJL model to be [25]  $B_{eff} = \Omega_{\text{int}}/V - B_0$  with  $B_0 V = \Omega_{\text{int}}|_{n_u=n_d=n_s=0}$  a constant value which makes the vacuum energy density zero. In this way, the thermodynamic potential can be expressed as  $\Omega = B_{eff} V + \Omega_{\text{FG}}$  which is to be compared to the MIT bag result  $\Omega = BV + \Omega_{\text{FG}}$ . Note, however, that  $\Omega_{\text{FG}}$  in the NJL model is calculated using the dynamical quark masses from Eq. (7).

Both PNS and neutron star matter are in beta equilibrium, which together with charge conservation implies

$$\mu_e - \mu_{\nu_e} = \mu_\mu - \mu_{\nu_\mu} ; \quad \mu_B = b_i \mu_n - q_i \mu_e + q_i \mu_{\nu_e} , \quad (9)$$

where  $b_i$  and  $q_i$  are the baryon number and charge, respectively, of the hadron or quark species  $i$ . We ignore surface and Coulomb effects for the structure in the mixed phase so the leptons are everywhere free Fermi gases.

The initial PNS contains trapped neutrinos, so the electron and muon lepton numbers may be assumed fixed:

$$Y_{L_e} \equiv \frac{n_e + n_{\nu_e}}{n_B} = 0.4; \quad Y_{L_\mu} \equiv \frac{n_\mu + n_{\nu_\mu}}{n_B} = 0. \quad (10)$$

Also, calculations generally show that the entropy of the inner half of the star has an entropy per baryon  $s \approx 1$ . In the cases in which the neutrinos have completely escaped, the neutrino chemical potentials and densities are vanishingly small. The departing neutrinos maximally heat the stellar interior to entropies around 2 per baryon after approximately 10–20 seconds [6–8]. After several minutes, neutrino cooling reduces the temperature to essentially zero on the scale of MeVs. Thus, we consider three approximate entropies and compositions to represent the thermodynamic conditions in an evolving PNS: the initial state ( $s = 1, Y_{L_e} = 0.4$ ), the maximally heated star ( $s = 2, Y_{\nu_e} = 0$ ), and the cold, catalyzed star ( $s = 0, Y_{\nu_e} = 0$ ). Of course, treating the PNS as a monolithic structure of fixed entropy and composition is an oversimplification, and full evolutionary calculations are required to confirm these estimates.

Quarks are assumed to appear by forming a mixed phase with the hadrons satisfying Gibbs' rules for phase equilibrium. Matter in this mixed phase is in thermal, mechanical and chemical equilibrium, so that

$$P^I = P^{II}; \quad \mu_n = 2\mu_d + \mu_u, \quad (11)$$

where  $I$  and  $II$  denote the hadronic and quark phases, respectively. The restriction that the pure phases I and II are independently charge neutral is replaced by the condition of global charge neutrality [1]

$$\chi n_c^I + (1 - \chi)n_c^{II} = 0, \quad (12)$$

where  $n_c$  is the charge density and  $\chi$  is the volume fraction of the hadronic phase. The energy and entropy densities in the mixed phase can be expressed in terms of the corresponding quantities in the hadronic and quark phases:

$$\varepsilon = \chi\varepsilon^I + (1 - \chi)\varepsilon^{II}, \quad s = \chi s^I + (1 - \chi)s^{II}. \quad (13)$$

The EOS for matter with hadrons is constructed with the MS model, and we considered models both with and without hyperons. In addition, we considered models incorporating a range of parameters  $\zeta$  and  $\xi$ . Two quark Lagrangians were selected, the NJL model with parameters given by [22] and the MIT bag model with  $150 \leq B/(\text{MeV fm}^{-3}) \leq 250$ .

The choice  $\zeta = \xi = 0$  maximizes the quark content of matter at a given density, since the hadronic EOS is stiffest for this case. This is illustrated in the left panels of Figure 1, which shows the hadron volume fraction  $\chi$  as a function of density for three representative hadronic parameter sets (neglecting hyperons) for cold matter without neutrinos. The NJL (MIT) quark model is shown in the upper (lower) panel. However, for a given stellar mass, the quark content of a neutron star is actually maximized for the softest parameter set  $\zeta = 0.06, \xi = 1.5$ , as shown in the right panels of Figure 1. This counterintuitive behavior occurs because the central densities achieved for a given stellar mass are greater for a softer EOS. Note that the maximum mass decreases with increasing softness of the hadronic EOS, which is as expected.

A more intuitive behavior results from variations in the parameters of the quark Lagrangian, which are explored in Figure 1. The parameters of the NJL model are relatively well constrained by experiment. However, the MIT bag model parameter  $B$  is only constrained by the requirement that the quark-hadron transition not occur too close to  $n_0$ , which implies that  $B$  is larger than about 125-150 MeV fm<sup>-3</sup>. The hadron volume fraction is displayed for the same hadronic parameters, but for different values of  $B$ , for the MIT bag model in Figure 2. The left panels show variations with density and the right panels show variations with stellar mass. The upper panels neglect hyperons while the lower panels include them. Smaller values for  $B$  result in a larger quark content at a given density, a larger quark content for a given stellar mass, and a smaller maximum mass. Note that there is little qualitative change produced by including hyperons.

In the remainder of this paper, we choose  $\zeta = \xi = 0$  for the hadronic parameters and  $B = 200$  MeV fm<sup>-3</sup> for the MIT bag constant. Figures 1 and 2 illustrate the qualitative changes in quark composition induced by parameter variations. It is clear that the mixed phase of quarks and hadrons can exist in neutron stars at least in the range of 1.2–2  $M_\odot$ , depending on the model. Ref. [26] concluded that the mixed phase is unlikely to exist in neutron stars with masses around 1.4  $M_\odot$  neutron stars, using the

NJL Lagrangian. However, this result appears to be dependent upon the hadronic interactions.

In the remainder of this paper, we shall consider in detail four EOSs: hadrons with and without hyperons for the NJL and MIT quark models.

The pressure of matter as a function of the density in units of  $n_0$ ,  $u = n_B/n_0$ , is shown in Figure 3 for these four cases. The mixed phase, indicated by thick lines, is marked by a pronounced softening of the EOS, observable as a large decrease in the incompressibility  $\partial P/\partial n$  of matter. The introduction of hyperons, or a large trapped neutrino fraction, suppresses the appearance of quarks for both quark models. The reason for this is that the additional contribution to the pressure from the neutrinos or the hyperons is more than cancelled by the addition of a degree of freedom to the system. A decrease in the pressure of the hadronic EOS forces the mixed phase to higher densities, because the hadronic pressure is not sufficient to match that of the quark phase until a higher density. Large amounts of trapped neutrinos produce a pronounced net increase in the pressure, however, because the (EOS-softening) transition is shifted to higher densities in all cases.

It is worth noting that the increase in pressure normally observed for finite-temperature matter compared to zero-temperature matter [8,10] is reversed in the mixed phase produced by quarks. This reversal does not occur for a mixed phase with kaon condensation [27]. This reversal originates in the fact that the phase transition begins at a lower density at finite temperature, so that the EOS softens at an earlier density. Even a small change in the threshold density of appearance for the mixed phase results in a significant net decrease of pressure at a fixed density.

The temperature as a function of baryon density for fixed entropy and net lepton concentration is presented in Figure 4, which compares the cases ( $s = 1, Y_{Le} = 0.4$ ) and ( $s = 2, Y_{\nu_e} = 0$ ). In addition to the cases in which quarks appear, the results ignoring quarks are also displayed for reference. The temperature for a multicomponent system in a pure phase can be analyzed by referring to the relation for degenerate Fermi particles

$$T = \frac{s}{\pi^2} \left( \sum_i \frac{\sqrt{p_{F,i}^2 + (m_i^*)^2}}{p_{F,i}^2} \right)^{-1}, \quad (14)$$

where  $m_i^*$  and  $p_{F,i}$  are the effective mass and the Fermi momentum of component  $i$ , respectively. This formula is quite accurate since the hadron and quark Fermi energies are large compared to the

temperature. The introduction of hyperons or quarks lowers the Fermi energies of the nucleons and simultaneously increases the specific heat of the matter, simply because there are more components. In the case of quarks, a further increase, which is just as significant, occurs due to the fact that quarks are rather more relativistic than hadrons. The combined effects for quarks results in an actual reduction of temperature with increasing density along an adiabat. These results are suggestive that the temperature will be smaller in a PNS containing quarks than in stars without quarks. The large reduction in temperature might also influence neutrino opacities, which are generally proportional to  $T^2$ . However, a PNS simulation is necessary to consistently evaluate the thermal evolution, since the smaller pressure of quark-containing matter would tend to increase the star's density and would oppose this effect.

The particle concentrations as functions of density are displayed in Figures 5 and 6 for the four EOSs considered here. The major difference that the choice of quark models produces concerns the concentration of the strange quark. The strange quark (dynamical) mass in the NJL model is much larger, by a factor of 2 to 3, than that assumed in the MIT bag model. This noticeably reduces its chemical potential, and hence its concentration, in the NJL model. The inclusion of hyperons does not produce significant changes to the nucleon or electron concentrations, although the electron concentration begins to fall at the threshold density for the appearance of hyperons which is lower than the low-density boundary of the mixed phase region. The muon concentration is generally much smaller than that of the electron and is omitted from the figures for the sake of clarity. By moving the mixed phase region to higher densities, the inclusion of hyperons, somewhat reduces the width of the mixed phase region. This is not apparent in the figures for the MIT bag case, however, because the mixed phase extends to rather large densities.

The mass-radius trajectories, computed from the standard relativistic stellar structure equations, are displayed in Figure 7 for the four EOSs and for the set of three thermodynamic conditions. Configurations in which the center of the star is in the mixed phase region are shown as bold lines. Although the results displayed are for a single parametrization of the hadronic matter, it is clear that neutron stars containing a mixed phase have a moderate range of masses. This range could be enhanced by altering either the hadronic or the quark matter EOS. The range of masses of stars containing a mixed

phase appears to be diminished in the case that hyperons exist, as noted in Refs. [3,26], but this result is somewhat dependent upon the hyperon coupling constants in addition to the hadronic and quark matter EOSs.

Coinciding with the result in Figure 3 that the quark-hadron transition at finite temperature occurs at a lower density than at zero temperature, and thereby reduces the pressure in the mixed-phase region, the neutrino-free stars with  $s = 2$  have smaller maximum masses than those for cold  $s = 0$  stars. Nevertheless, the pressure in the range  $n_0 < n < 1.5n_0$  increases with entropy. This increase in pressure results in larger stellar radii for stars below the maximum mass, a result consistent with the general results found by Ref. [28]. The difference of pressures between the ( $s = 0, Y_{Le} = 0.4$ ) and ( $s = 1, Y_{\nu_e}$ ) cases is much smaller, and produces relatively less of a radius change.

It is immediately apparent that in all cases shown, a range of masses are metastable, a condition which exists if the initial PNS configuration has a greater maximum mass than the final configuration [3]. This result was foreshadowed by the results presented in Figure 3, in which the pressure for the lepton-rich configuration was much larger in the mixed phase than for the other configurations. In addition, as the neutrinos diffuse from the star, the mixed phase shifts to lower densities and so a greater proportion of the center of the star is in the mixed phase. In the cases shown, the maximum mass occurs when the star's central density is in the mixed phase region. In other words, pure quark configurations seem unlikely to occur.

This last point is highlighted in Figure 8 which shows phase diagrams for the mixed phase in the baryon density-neutrino fraction plane. The upper and lower boundaries of the mixed phase region are displayed as bold lines, while the central densities of the maximum mass configurations are shown as light lines. In no case, for either quark model and whether or not hyperons are included, are pure quark stars possible. The high-density phase boundaries are always well above the central densities.

In summary, it is possible for a mixed phase to exist in a neutron star of virtually any mass above  $1.4 M_{\odot}$ . Depending upon the EOSs, a mixed phase is more likely to exist in stars larger than  $1.5 M_{\odot}$ . The precise stellar mass above which a mixed phase containing quarks might exist depends on the “softness” of the hadronic EOS and the effective bag pressure of the quark model. Although the quark content of matter at a given *density* is maximized for stiffer hadronic equations of state, the extent of

the mixed phase region in a neutron star of a given mass is maximized for softer hadronic EOSs. We have shown that only in extreme cases could a pure quark star result.

This mixed phase is delayed until most neutrinos have diffused from the star, leading to the possible metastability of PNSs, a robust result which depends only on the existence of quarks in dense matter. Finite temperature permits the quark-hadron transition to occur at slightly lower densities than at zero temperature, but in a newly-formed PNS this effect is swamped by the large trapped neutrino fraction which has the opposite tendency. Furthermore,  $\partial T/\partial n < 0$  along adiabats in the quark-hadron mixed phase, a behavior opposite to that generally found in a mixed phase region containing a kaon condensate. This implies that core temperatures may be significantly lower in stars containing quarks than in those not containing quarks. Neutrino opacities, which are sensitive to temperature, will be affected, but the implications for the emitted neutrino fluxes and temperatures can only be reliably evaluated in the context of a full PNS simulation.

We acknowledge the support of the U.S. Department of Energy under contracts DOE/DE-FG02-88ER-40388 (AS and MP) and DOE/DE-FG02-87ER-40317 (JML).

## REFERENCES

- [1] N. K. Glendenning. *Phys. Rev. D*, 46:1274, 1992.
- [2] H. Heiselberg, C. J. Pethick, and E. F. Staubo. *Phys. Rev. Lett.*, 70:1355, 1993.
- [3] M. Prakash, J. R. Cooke, and J.M. Lattimer. *Phys. Rev. D*, 52:661, 1995.
- [4] Quark Matter '99. *Nucl. Phys. A*, 661:1–765, 1999.
- [5] T. J. Burrows, A. Mazurek and J. M. Lattimer. *Astrophys. J.*, 251:325, 1981.
- [6] A. Burrows and J. M. Lattimer. *Astrophys. J.*, 307:178, 1986.
- [7] W. Keil and H. T. Janka. *Astron. Astrophys.*, 296:145, 1995.
- [8] J. A. Pons, S. Reddy, M. Prakash, J. M. Lattimer, and J. A. Miralles. *Astrophys. J.*, 513:780, 1999.
- [9] V. Thorsson, M. Prakash, and J. M. Lattimer. *Nucl. Phys. A*, 572:693, 1994.
- [10] M. Prakash, I. Bombaci, Manju Prakash, P. J. Ellis, J. M. Lattimer, and R. Knorren. *Phys. Rep.*, 280:1, 1997.
- [11] P. J. Ellis, J. M. Lattimer, and M. Prakash. *Comm. Nuc. Part. Phys.*, 22:63, 1996.
- [12] H. Müller and B. D. Serot. *Nucl. Phys. A*, 606:508, 1996.
- [13] J. W. Negele and D. Vautherin. *Nucl. Phys. A*, 207:298, 1974.
- [14] G. Baym, C. J. Pethick, and P. Sutherland. *Astrophys. J.*, 170:299, 1971.
- [15] N. K. Glendenning and S. A. Moszkowski. *Phys. Rev. Lett.*, 61:2414, 1991.
- [16] D. J. Millener, C. B. Dover, and A. Gal. *Phys. Rev. C*, 38:2700, 1988.
- [17] R. Knorren, M. Prakash, and P. J. Ellis. *Phys. Rev. C*, 52:3470, 1995.
- [18] J. I. Kapusta. *Finite-Temperature Field Theory*. Cambridge University Press, Cambridge, U. K., 1985.

- [19] Manju Prakash, E. Baron, and M. Prakash. *Phys. Lett. B*, 243:175, 1990.
- [20] Y. Nambu and G. Jona-Lasinio. *Phys. Rev.*, 122:345, 1961.
- [21] G. 't Hooft. *Phys. Rep.*, 142:357, 1986.
- [22] P. Rehberg, S. P. Klevansky, and J. Hüfner. *Phys. Rev. C*, 53:410, 1996.
- [23] T. Kunihiro. *Phys. Lett. B*, 219:363, 1989.
- [24] T. Hatsuda and T. Kunihiro. *Phys. Rep.*, 247:221, 1994.
- [25] M. Buballa and M. Oertel. *Phys. Lett. B*, 457:261, 1999.
- [26] K. Schertler, S. Leupold, and J. Schaffner-Bielich. *Phys. Rev. C*, 60:025801, 1999.
- [27] J. A. Pons, S. Reddy, P.J. Ellis, M. Prakash, and J.M. Lattimer. *Phys. Rev. C*, submitted, 2000.
- [28] J.M. Lattimer and M. Prakash. *Astrophys. J.*, submitted, 2000.

## FIGURE CAPTIONS

Figure 1: Left panels: The volume fraction of hadrons as a function of density in units of  $n_0$  within the quark-hadron mixed phase for cold, catalyzed matter ( $s = 0, Y_{\nu_e} = 0$ ) without hyperons (npQ). Three choices for the parameters  $\zeta$  and  $\xi$  in the Müller-Serot (MS) hadronic Lagrangian are illustrated, and the upper panel refers to the Nambu Jones-Lasinio (NJL) model and the lower panel to the MIT bag model with  $B = 200 \text{ MeV fm}^{-3}$ . Right panels: The volume fraction of hadrons in the star's center as a function of stellar mass for the same configurations and quark models.

Figure 2: The same as Figure 1, except that results are compared for three choices of the bag constant  $B$  (in units of  $\text{MeV fm}^{-3}$ ) in the MIT bag model. Hyperons are ignored in the top panels (npQ) and included in the bottom panels (npHQ). The parameters  $\zeta = \xi = 0$  in the Müller-Serot (MS) hadronic Lagrangian are chosen.

Figure 3: Pressure versus density in units of  $n_0$  for three representative snapshots during the evolution of a proto-neutron star. The top (bottom) panels display results without (with) hyperons, and the left (right) panels utilize the NJL (MIT bag) quark EOS. The parameters  $\zeta = \xi = 0$  in the Müller-Serot (MS) hadronic Lagrangian are chosen. Bold curves indicate the mixed phase region.

Figure 4: Temperature versus density in units of  $n_0$  for two PNS evolutionary snapshots. The upper (lower) panel displays results for the NJL (MIT bag) Lagrangian. The parameters  $\zeta = \xi = 0$  in the Müller-Serot (MS) hadronic Lagrangian are chosen. Results are compared for matter containing only nucleons (np), nucleons plus hyperons (npH), nucleons plus quarks (npQ) and nucleons, hyperons and quarks (npHQ). Bold curves indicate the mixed phase region.

Figure 5: The concentrations of hadrons, quarks, and leptons as functions of density in units of  $n_0$ . Three representative snapshots during the evolution of a proto-neutron star are displayed. Matter is assumed to contain nucleons and quarks (npQ). The parameters  $\zeta = \xi = 0$  in the Müller-Serot (MS)

hadronic Lagrangian are chosen. Bold curves indicate the mixed phase region.

Figure 6: The same as Figure 5, except that hyperons are included (npHQ).

Figure 7: The gravitational mass versus radius, for three representative snapshots during the PNS evolution. The left (right) panels are for the NJL (MIT bag) quark EOS, and hyperons are (are not) included in the bottom (top) panels. The parameters  $\zeta = \xi = 0$  in the Müller-Serot (MS) hadronic Lagrangian are chosen. Bold lines indicate configurations with a mixed phase at the star's center.

Figure 8: The phase diagram of the quark-hadron transition in the baryon number density - neutrino concentration plane for three representative snapshots during the evolution of a proto-neutron star. The left (right) panels are for the NJL (MIT bag) quark EOS, and hyperons are (are not) included in the bottom (top) panels. The parameters  $\zeta = \xi = 0$  in the Müller-Serot (MS) hadronic Lagrangian are chosen. The lower- and upper-density boundaries of the mixed phase are indicated by bold curves. The central densities of maximum mass configurations are shown by thin curves.

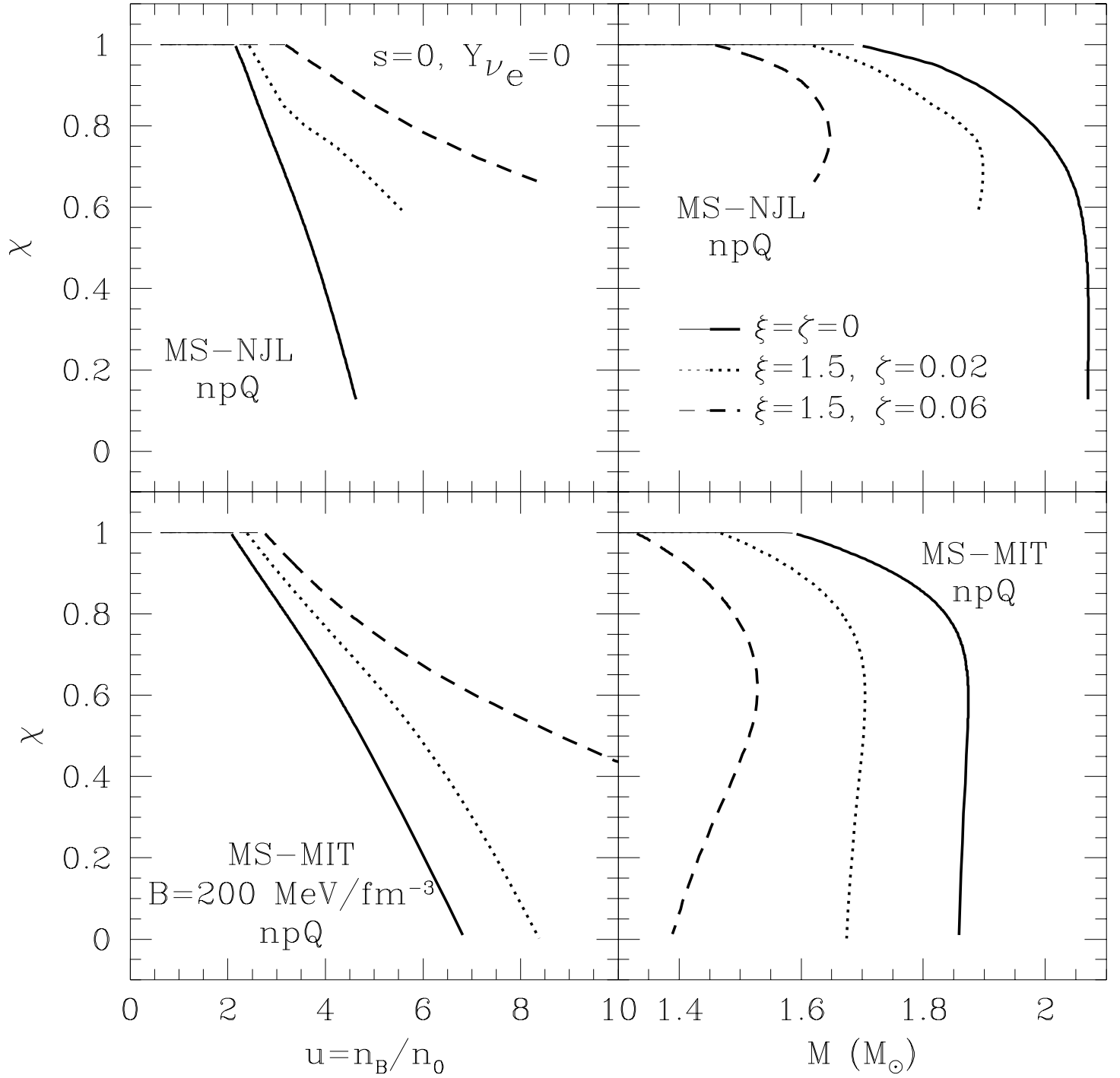


FIG. 1.

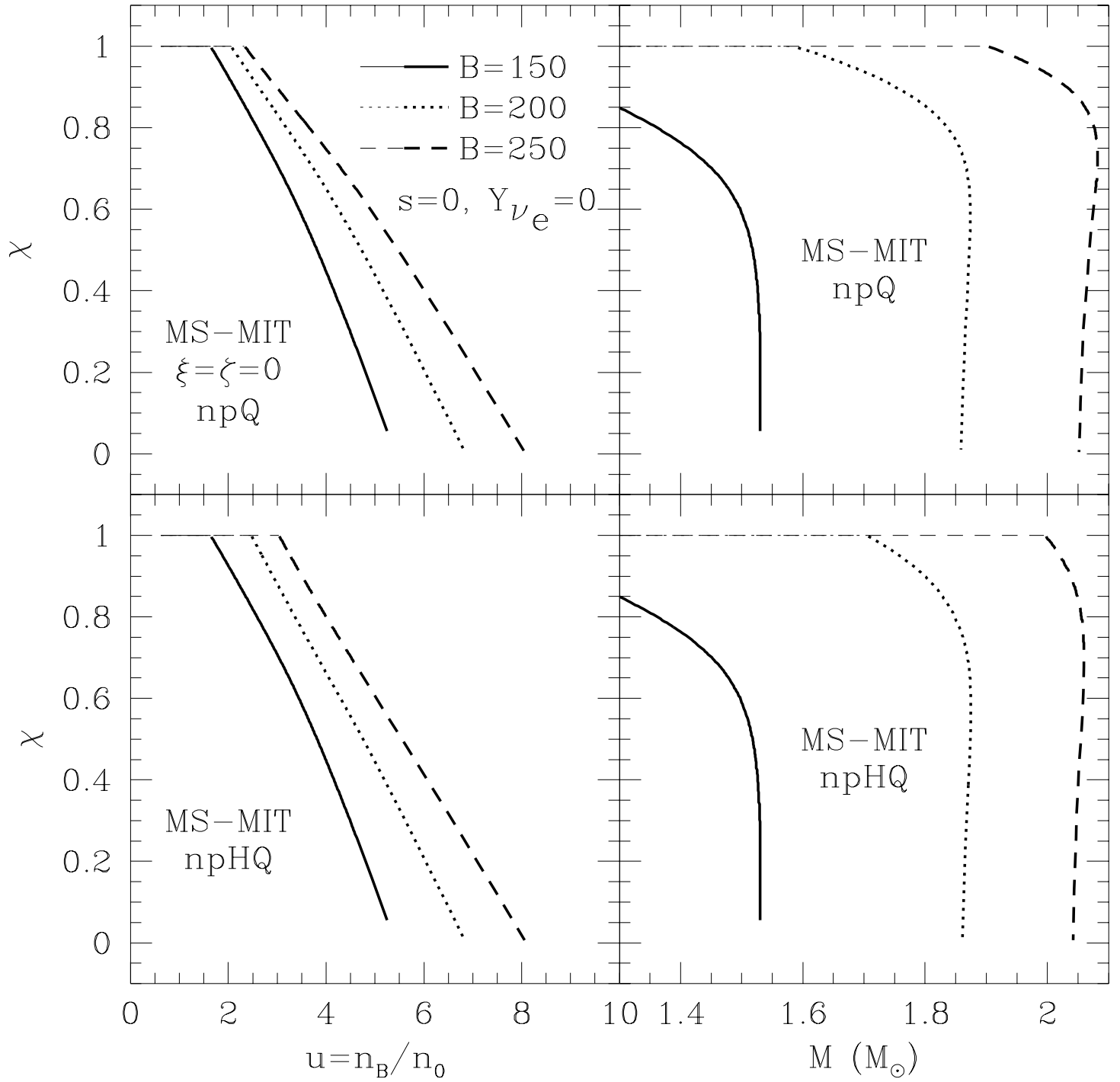


FIG. 2.

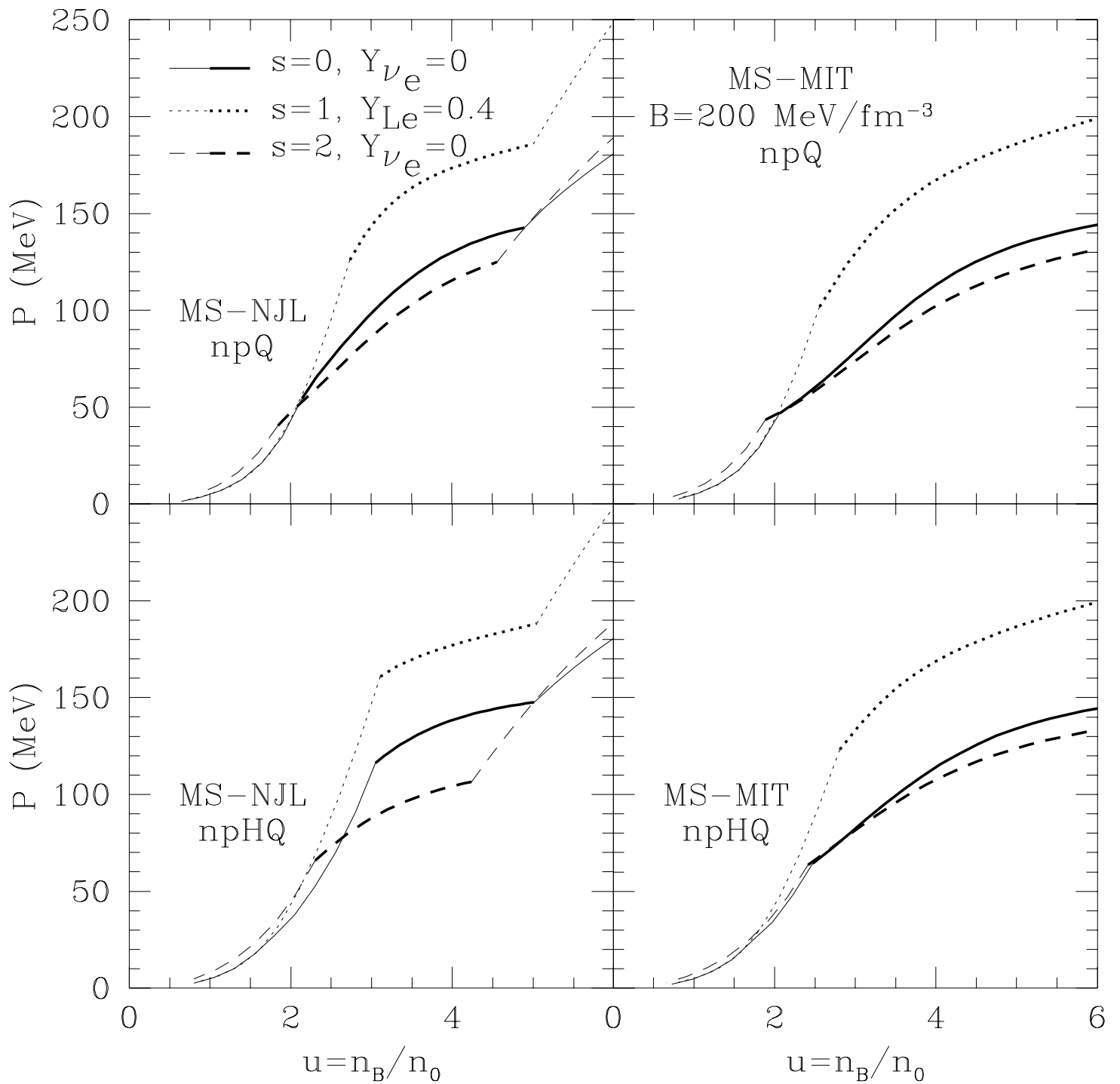


FIG. 3.

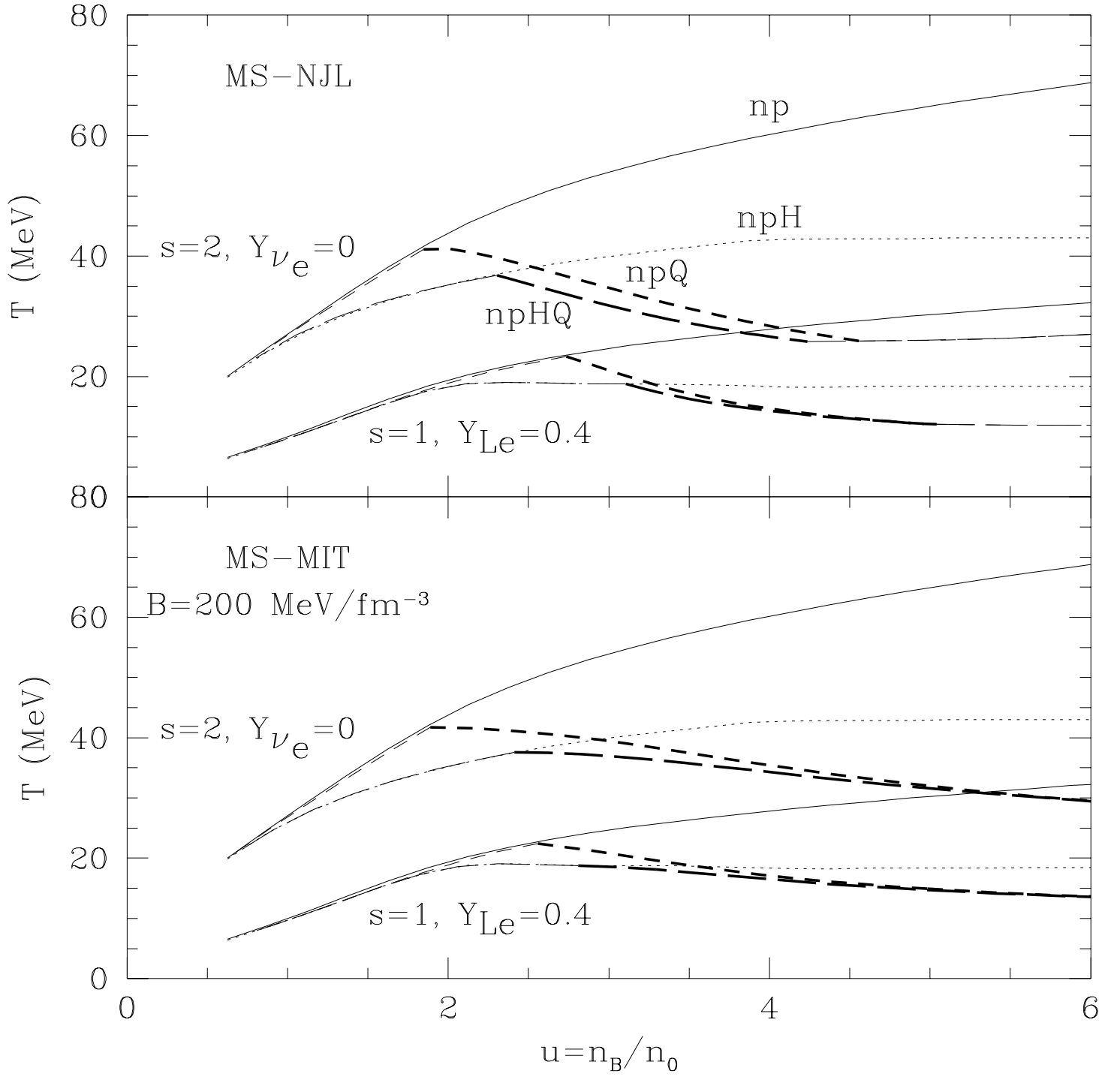


FIG. 4.

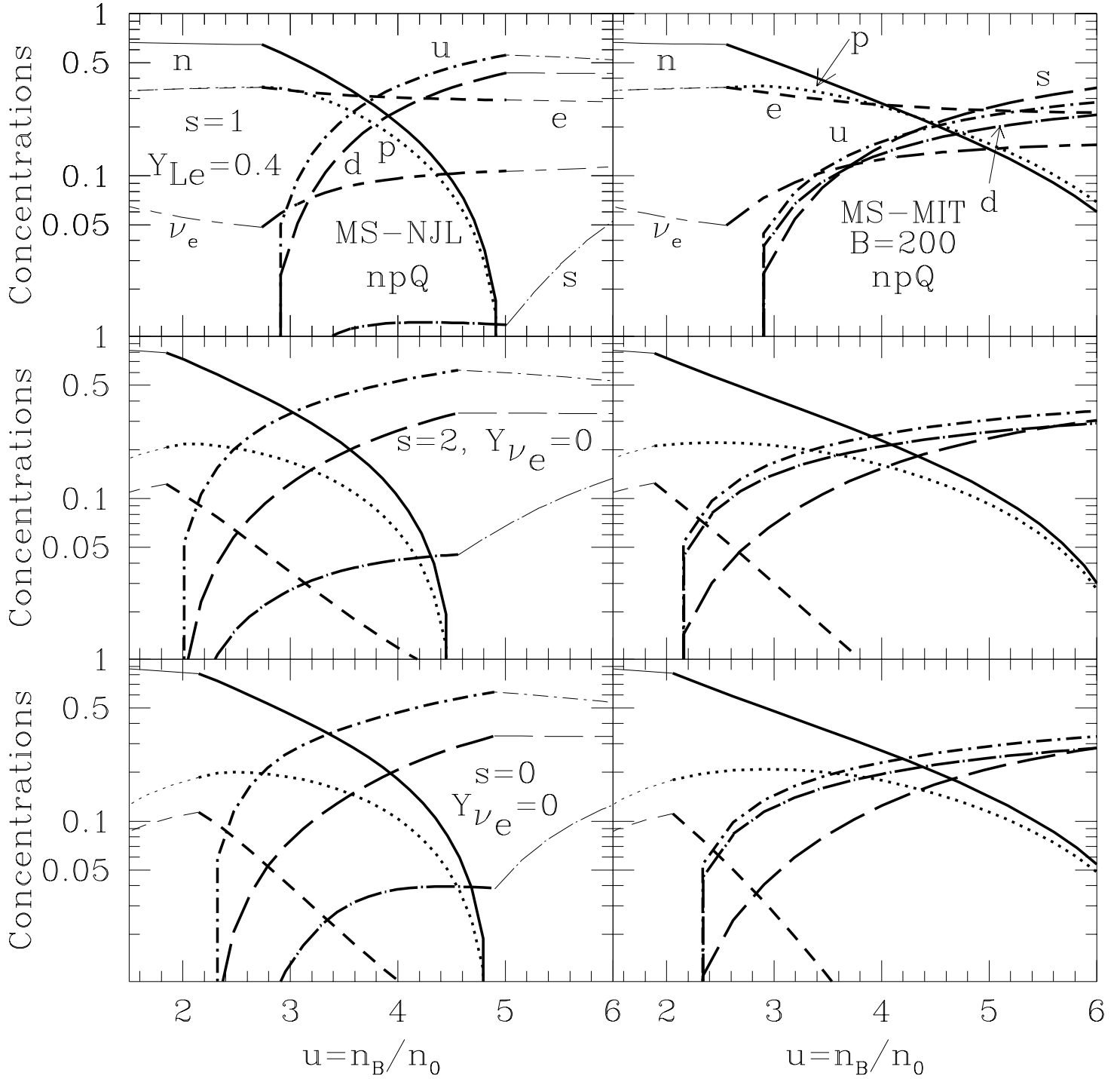


FIG. 5.

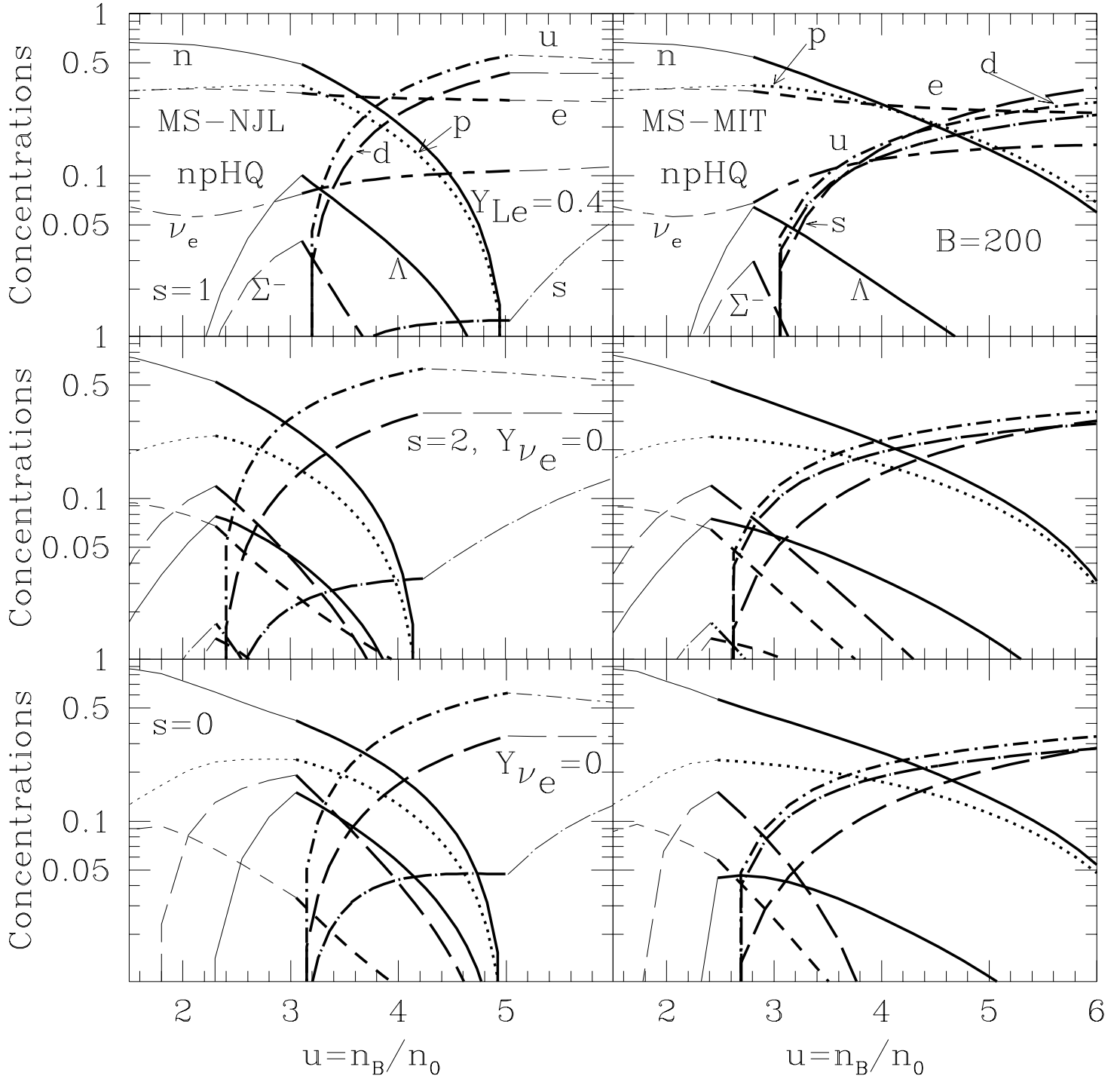


FIG. 6.

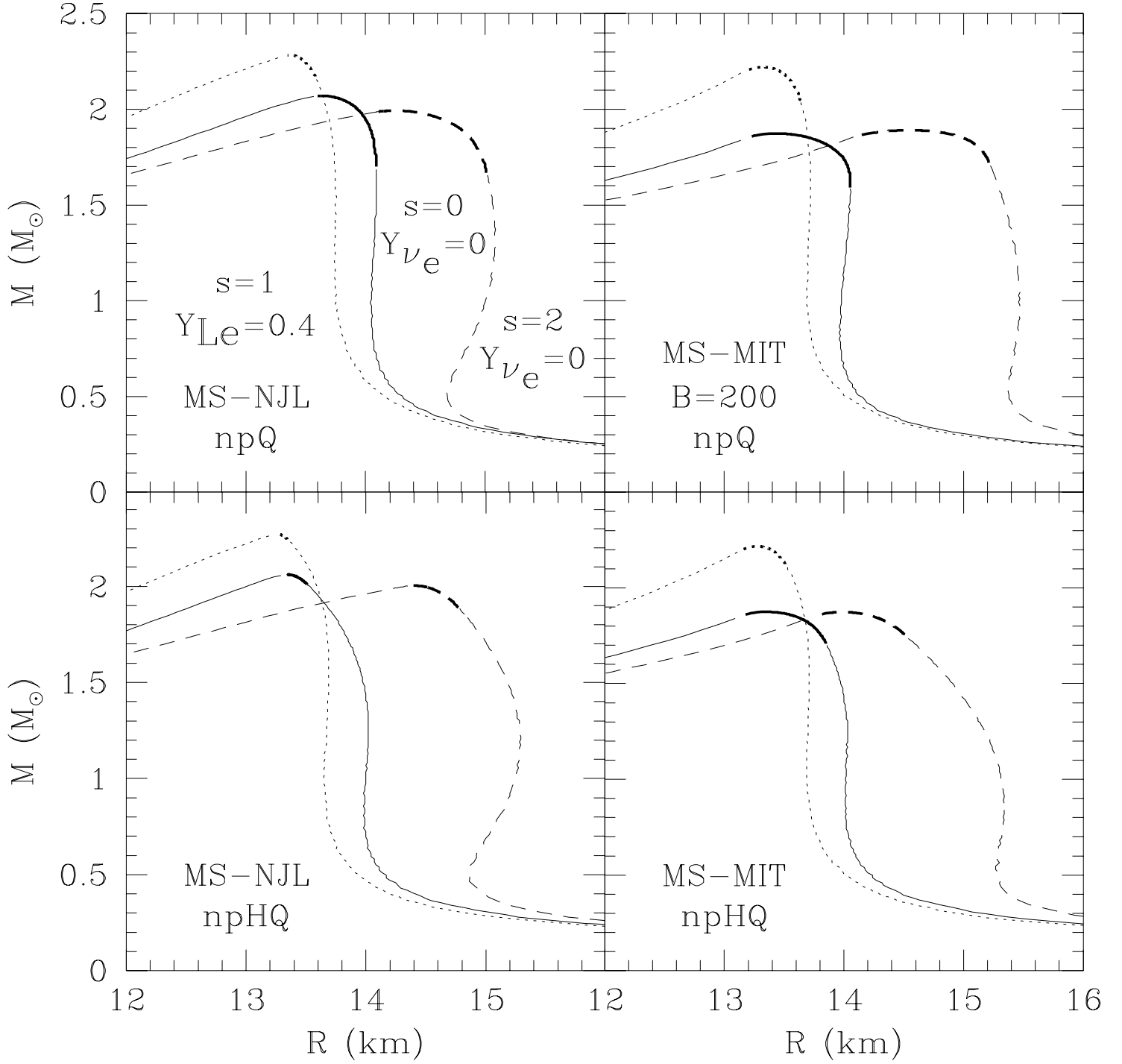


FIG. 7.

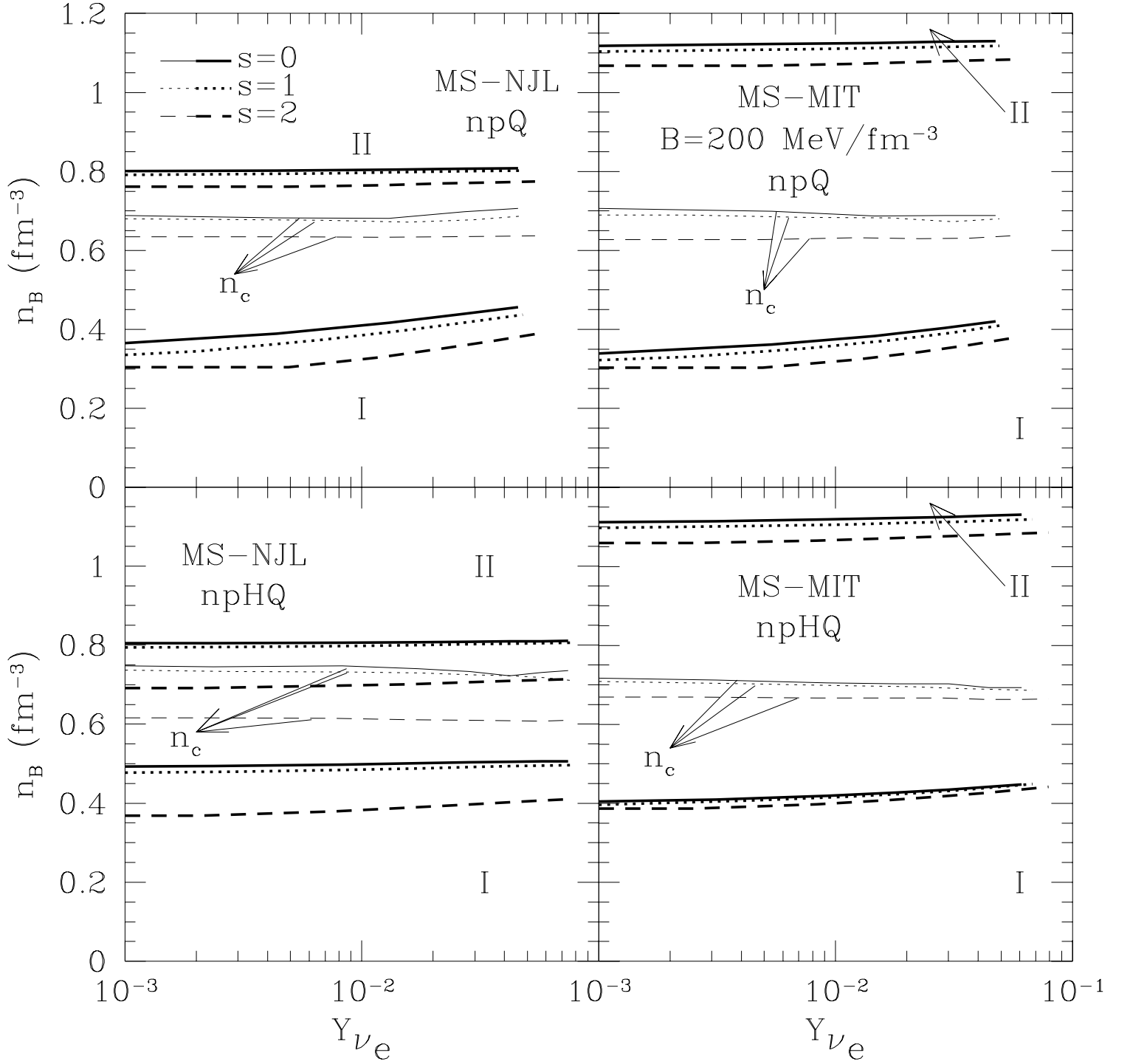


FIG. 8.